Nonlinear Predictive Control Applied to Steam/Water Loop in Large Scale Ships

Shiquan Zhao[1,2,3], Ricardo Cajo[1,3,4] Robin De Keyser[1,3], Sheng Liu[2], Clara M. Ionescu[1,3,5]

[1]*Faculty of Engineering and Architecture, Ghent University*
Research group on Dynamical Systems and Control, Technologiepark 914, B9052 Zwijnaarde, Belgium
(email: Shiquan.Zhao@UGent.be)
[2]*College of Automation, Harbin Engineering University, China*
[3]*Core Lab EEDT- Energy Efficient Drive Trains, Flanders Make*
[4]*Grupo de Investigación en Automatización y Control Industrial, Campus Gustavo Galindo*
Km 30.5 Vía Perimetral, P.O. Box 09-01-5863, Guayaquil, Ecuador
[5]*Technical University of Cluj Napoca, Department of Automatic Control, Memorandumului Street no 28, Cluj, Romania*

Abstract: In steam/water loop for large scale ships, there are mainly five sub-loops posing different dynamics in the complete process. When optimization is involved, it is necessary to select different prediction horizons for each loop. In this work, the effect of prediction horizon for Multiple-Input Multiple-Output (MIMO) system is studied. Firstly, Nonlinear Extended Prediction Self-Adaptive Controller (NEPSAC) is designed for the steam/water loop system. Secondly, different prediction horizons are simulated within the NEPSAC algorithm. Based on simulation results, we conclude that specific tuning of prediction horizons based on loop's dynamic outperforms the case when a trade-off is made and a single valued prediction horizon is used for all the loops.

Keywords: Nonlinear predictive control, Prediction horizon, Steam power plant, Steam/water loop, Multi-Input and Multi-Output

1. INTRODUCTION

The steam power plant system in large scale ships has some challenging and typical features, from which we enumerate a few: a complex system structure, large number of equipment, complicated coupling relationships in variables and a severe time delay. During the operation of large scale ships, there are seven operating points and six processes about operating points conversion (Liu, 2006). Although a rich experience in steam power plant designing and operating is available, the optimization of both equipment features and system dynamics are still in the beginning phase. In order to improve the dynamic performance of steam power plant in large scale ships and ensure it works safely, the research on advanced control strategies for steam power plants has great significance and potential.

The steam/water loop is one of the most important part in steam power plant. In this complex process, there are five sub-loops existing in steam/water loop: i) drum water level control loop, ii) deaerator water level control loop, iii) deaerator pressure control loop, iv) condenser water level control loop and v) exhaust manifold pressure control loop. The controller design for steam/water loop in large scale ships is a challenging process control problem. The time delay is present in many sub-loops in this system. Hence, the model predictive control (MPC) is used for its superiority in dealing with time delay and constraints (Morari, and Lee, 1999; Folea et al., 2016). An economic model predictive controller is developed in (Liu and Cui, 2018). It directly utilizes the economic index of boiler-turbine system as the cost function and realizes the economic optimization as well as the dynamic tracking. An adaptive grey predictor based algorithm to boiler drum level control was proposed (Yu et al., 2006) to deal with the challenging issues: i) effect of "false water level", ii) control parameter mismatches due to variant working conditions, and iii) signal noise caused by uncertainties of drum level. Nonlinear multivariable hierarchical model predictive control (HMPC) for boiler-turbine system was proposed (Kong et al., 2015). Both the economic performance and the regulatory criterion are defined in the objective function of the upper layer of the HMPC scheme and obvious improvement in economic performance and computation time is obtained. Other MPC methods are also studied for the power plant (Sindareh-Esfahani et al., 2017; Ławryńczuk, 2017; Wu et al., 2014).

The methods introduced above are mainly for the boiler in the steam/water loop. However, in this paper we include analysis on all five sub-loops, composed of two fast processes (control loops for the pressure in deaerator and exhaust manifold) and three slow processes (control loops for the water level in drum, deaerator and condenser). Hence, it is necessary to discuss the influence of prediction horizon for different loops. The literature shows that higher values in the prediction horizon resulted in better performance (Debert et al., 2010), at the cost of extra computational effort. However, we believe the horizon needs to be tailored according to the dynamics of the plant, which in our case vary significantly
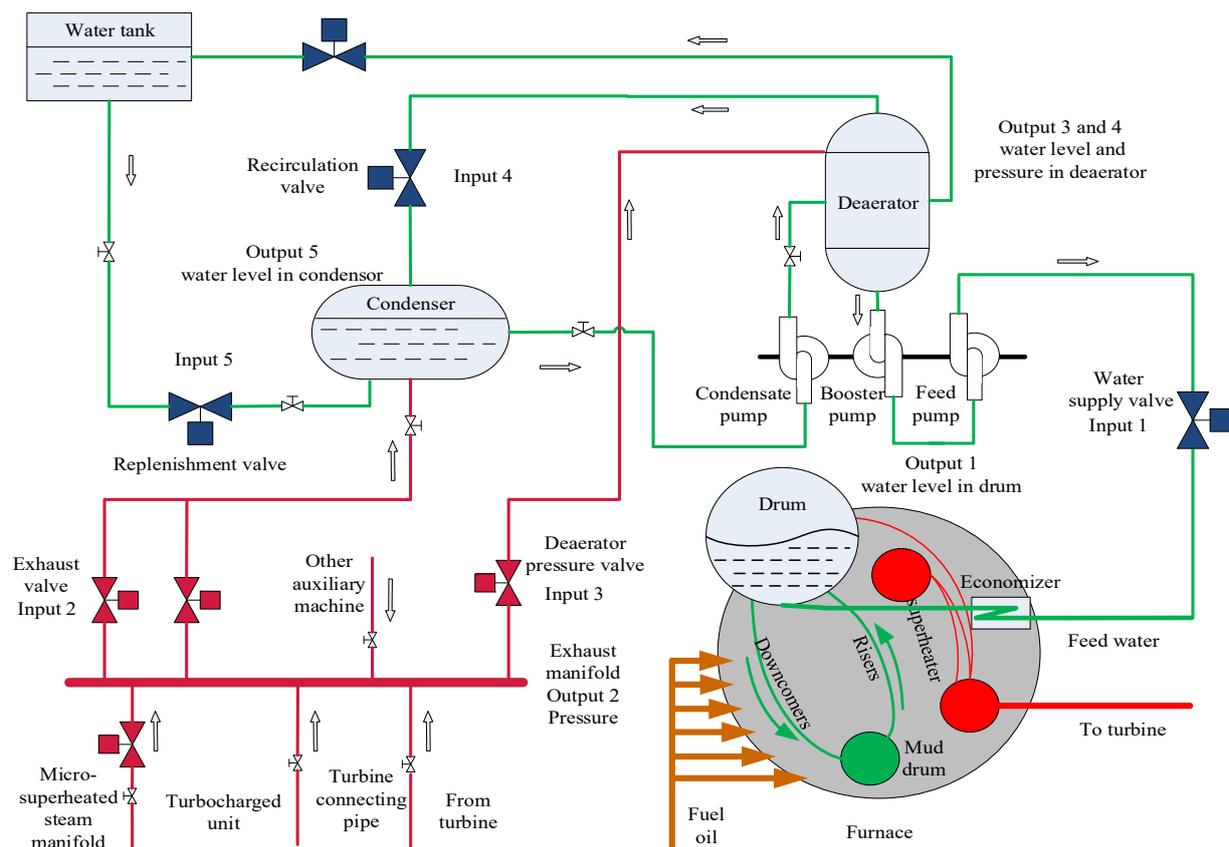
Fig. 1. Scheme of complete steam/water loop investigated in this paper

between the loops. At the same time, the presence of five sub-loops and the strong interaction between them, makes the explicit form of this system numerically instable, increasing the difficulty to design the MPC scheme. The advantage of NEPSAC is that it does not work with state space forms, prone to numerical properties and conditions, but with input-output filtering techniques (Hernandez et al., 2016). Therefore, in this paper the NEPSAC method is applied to steam/water loop, and different prediction horizons are selected and analysed.

The paper is structured as follows. The model of steam/water loop is obtained in section 2. A very brief introduction about NEPSAC is described in section 3. The results and discussion are given in section 4 and a conclusion section points to the next steps.

2. MODEL OF THE STEAM/WATER LOOP

The scheme of steam/water loop is schematically depicted in Fig. 1, with the main five sub-loops. It includes the boiler, the deaerator, the condenser and the exhaust manifold. There are two main loops, one for steam indicated by red line, another one for water indicated by the green line. The system works as follows. Firstly, the water from water tank goes to condenser. Secondly, the water will be deoxygenated in the deaerator and be pumped to boiler. Due to a higher density of feed water, it goes into the mud drum. After being heated in the risers, the feed water turned into mixture of steam and water. Thirdly, steam gets separated from mixture and heated in the superheater. Finally, the steam with a certain pressure and temperature services for the steam turbine. The used

steam will be sent back to exhaust manifold and most of the steam gets condensed in the condenser, while the remaining part services in the deaerator for deoxygenation.

The sources of these models for each equipment are described as follows. The nonlinear model of the boiler comes from (Åström and Bell, 2000); the model of exhaust manifold is approximated as a second-order model plus a delay item according to (Wang et al., 2014); the models of deaerator and condenser are obtained according to (Wang et al., 2015). In order to illustrate the nonlinearity of the system, staircase tests are performed on each sub-loops in the system with 10% changes for each step. The results for the first loop is shown in Fig. 2.
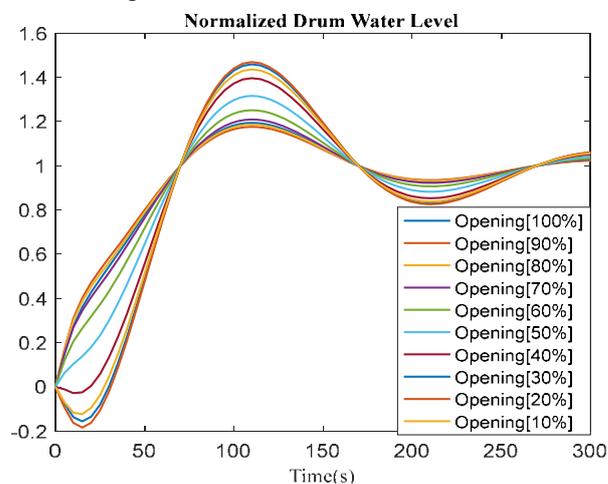

Fig. 2. Normalized drum water level in staircase test

The parameters involved in this paper are shown in Table 1, including the operating points and range of outputs variables (water level of drum, pressure in exhaust manifold, water level and pressure in deaerator and water level of condenser). The inputs in steam/water loop are the opening of valves (water supply valve, exhaust valve, deaerator pressure valve, recirculation valve and replenishment valve).

Table 1. Parameters used in steam/water loop

Output variables	Operating points	Range	Units
Drum water level	1.774	1.39-2.19	m
Exhaust manifold pressure	101	87.03-133.8	KPa
Deaerator pressure	32.55	24.9-43.86	KPa
Deaerator water level	0.6839	0.489–0.882	m
Condenser water level	0.3859	0.32-0.63	m

3. NONLINEAR MODEL PREDICTIVE CONTROL

In the case of application of model predictive control to nonlinear systems, the principle of superposition is not applicable any more. In this paper, the NEPSAC (Nonlinear Extended Prediction Self-Adaptive Control) methodology is chosen because it does not linearize the model, but it uses an iterative approach at each moment in time to bypass the superposition principle and compute the optimal inputs (Castano et al., 2015). By using iterative convergence to find a δU near to zero (δU is part of the optimal input at this moment), the method can be directly applied to nonlinear systems.

The description of the flow chart of NEPSAC follows. Consider a nonlinear system described below.

$$y(t) = x(t) + n(t) \tag{1}$$

where $y(t)$ indicates the measured output of system; $x(t)$ is the output of model and $n(t)$ is the model/process disturbance. The output of the model $x(t)$ depends on the past outputs and inputs, and can be expressed generically as:

$$x(t) = f[x(t-1), x(t-2),\ldots,u(t-1),u(t-2),\ldots] \tag{2}$$

The output in EPSAC for future consists of two parts:

$$u(t+k \,|\, t) = u_{base}(t+k \,|\, t) + \delta u(t+k \,|\, t) \tag{3}$$

where $u_{base}(t+k\,|\,t)$ indicates basic future control scenario and $\delta u(t+k\,|\,t)$ indicates the optimizing future control actions. The following results will be obtained according to these control effort.

$$y(t+k \,|\, t) = y_{base}(t+k \,|\, t) + y_{opt}(t+k \,|\, t) \tag{4}$$

where $y_{base}(t+k\,|\,t)$ is the effect of base future control and $y_{opt}(t+k\,|\,t)$ is the effect of optimizing future control actions $\delta u(t\,|\,t)$, ... , $\delta u(t+N_u-1\,|\,t)$. The part of $y_{opt}(t+k\,|\,t)$ can be expressed as a discrete time convolution as follows:

$$y_{opt}(t+k \,|\, t) = h_k \delta u(u \,|\, t) + h_{k-1}\delta u(t+1 \,|\, t) + \ldots$$
$$+ g_{k-N_u+1}\delta u(t+N_u-1 \,|\, t) \tag{5}$$

where $h_1, \ldots h_{N_2}$ are impulse response coefficients and $g_1, \ldots g_{N_2}$ are the step response coefficients, and thus the following formulation can be obtained:

$$\mathbf{Y} = \bar{\mathbf{Y}} + \mathbf{GU} \tag{6}$$

where, $\mathbf{Y} = [y(t+N_1 \,|\, t) \ldots y(t+N_2 \,|\, t)]^T$ $\mathbf{U} = [\delta u(t \,|\, t) \ldots \delta u(t+N_u-1 \,|\, t)]^T$
$\bar{\mathbf{Y}} = [y_{base}(t+N_1 \,|\, t) \ldots y_{base}(t+N_2 \,|\, t)]^T$, and

$$\mathbf{G} = \begin{bmatrix} h_{N_1} & h_{N_1-1} & \cdots & g_{N_1-N_u+1} \\ h_{N_1+1} & h_{N_1} & \cdots & \cdots \\ \cdots & \cdots & \cdots & \cdots \\ h_{N_2} & h_{N_2-1} & \cdots & g_{N_2-N_u+1} \end{bmatrix} \tag{7}$$

In order to apply NEPSAC for MIMO system, the individual error of each output is minimized separately. The objective function is as follows for our system with five sub-loops.

$$\sum_{k=N_1}^{N_2} [r_i(t+k \,|\, t) - y_i(t+k \,|\, t)]^2 \tag{8}$$

By defining $\mathbf{G}_{ik}$ as the influence from kth input to ith output, Eq. (8) can be rewritten as:

$$(\mathbf{R}_i - \mathbf{Y}_i)^T(\mathbf{R}_i - \mathbf{Y}_i) = (\mathbf{R}_i - \bar{\mathbf{Y}}_i - \sum_{k=1}^{5}\mathbf{G}_{ik}\mathbf{U}_k)^T(\mathbf{R}_i - \bar{\mathbf{Y}}_i - \sum_{k=1}^{5}\mathbf{G}_{ik}\mathbf{U}_k) \tag{9}$$

with: $\begin{cases} \mathbf{R}_i = [r_i(t+N_1 \,|\, t) \ldots r_i(t+N_2 \,|\, t)]^T \\ \mathbf{Y}_i = [y_i(t+N_1 \,|\, t) \ldots y_i(t+N_2 \,|\, t)]^T \end{cases}$ $(i = 1,\ldots,5)$

Taking constraints from inputs and outputs into account. The process to find the minimum cost function becomes an optimization problem which is called quadratic programming.

$$\min_{\mathbf{U}_i} \mathbf{J}_i(\mathbf{U}_i) = \mathbf{U}_i^T \mathbf{H}_i \mathbf{U}_i + 2\mathbf{f}_i^T \mathbf{U}_i + c_i \quad \text{subject to } \mathbf{AU} \leq \mathbf{b} \tag{10}$$

with $\begin{cases} \mathbf{H}_i = \mathbf{G}_{ii}^T \mathbf{G}_{ii} \qquad \mathbf{f}_i = -\mathbf{G}_{ii}^T(\mathbf{R}_i - \bar{\mathbf{Y}}_i - \sum_{k=1}^{5}\mathbf{G}_{ik}\mathbf{U}_k) \\ c_i = (\mathbf{R}_i - \bar{\mathbf{Y}}_i - \sum_{k=1}^{5}\mathbf{G}_{ik}\mathbf{U}_k)^T(\mathbf{R}_i - \bar{\mathbf{Y}}_i - \sum_{k=1}^{5}\mathbf{G}_{ik}\mathbf{U}_k) \end{cases}$

where $\mathbf{A}$ is a matrix and $\mathbf{b}$ is a vector according to the constraints. By solving the quadratic problem, the optimal $\mathbf{U}$ can be obtained.

Actually, this is only valid for linear system. In order to apply this linear model predictive control to nonlinear case, the effect of optimizing future control can be removed iteratively by making $\delta u(t+k\,|\,t)$ smaller tends to zero. The principle of NEPSAC is shown in Fig. 3 by means of a flow chart. And the procedure of NEPSAC can be summarized as follows.

1). Select an initial $\{u_{base}(t+k\,|\,t), k = 0\ldots N_u-1\}$, and this should be as close as possible to the optimal strategy $u(t+k\,|\,t)$, which means $\delta u(t+k\,|\,t)$ is close to zero and thus the term $y_{opt}(t+k\,|\,t)$ is also close to zero. In this paper, $u_{base}(t+k\,|\,t) \equiv u(t+k\,|\,t-1)$ is chosen.
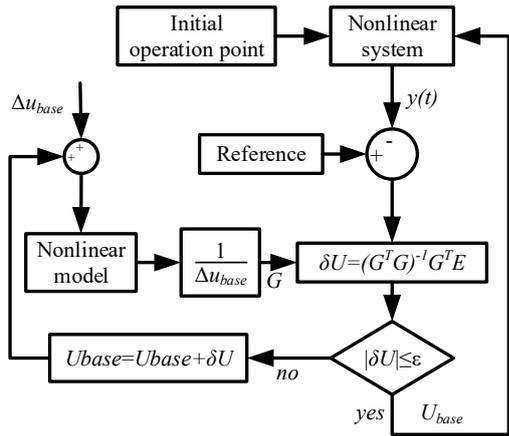
Fig. 3. Flow chart representation of NEPSAC principles

2). After choose the $\{u_{base}(t+k\,|\,t), k=0...N_u-1\}$, and calculate the $\{\delta u(t+k\,|\,t), k=0...N_u-1\}$, $u(t+k\,|\,t)$ is obtained. At the moment $u(t+k\,|\,t)$ is not the final optimal results due to the $\delta u(t+k\,|\,t)$ is not close to zero enough (indicated as ε).

3). Take the $u(t+k\,|\,t)$ from step 2 as a new $u_{base}(t+k\,|\,t)$, and calculate $\delta u(t+k\,|\,t)$ again.

4). Repeat step 2 and 3 until the item $\delta u(t+k\,|\,t)$ is as close as possible to zero, which means the superposition principle is no longer involved. The final obtained control signal $u(t+k\,|\,t)$ will be the optimal inputs for the system.

4. SIMULATION RESULTS AND ANALYSIS

In this section, the NEPSAC method is applied to the complete steam/water loop, and the performance with different prediction horizon sets are compared. Next, step tests over the entire operating range are applied to test the robustness of this algorithm.

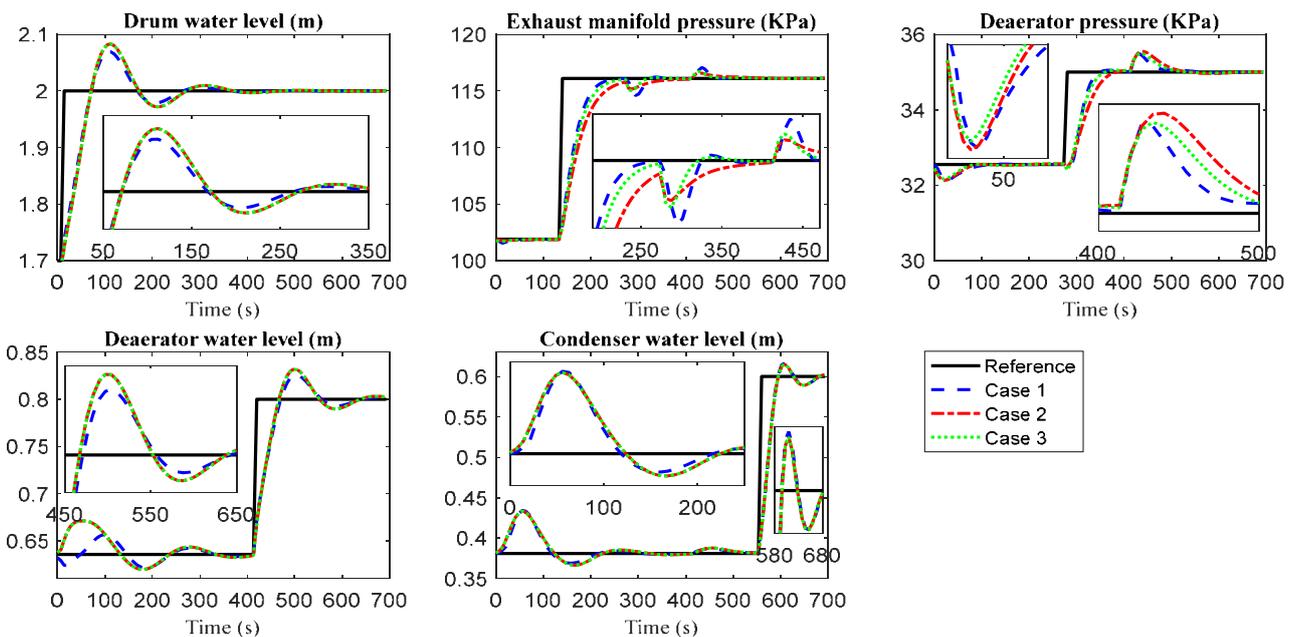### 4.1 Performance with Different Prediction Horizon Sets

According to open loop tests for steam/water loop, the settling time for different sub-loops are 200s, 100s, 70s, 170s and 170 s, respectively. As a rule, the control loop rate should be at least ten times faster than the time constant of the system. Hence, the sampling period for this system is chosen as 7 s. Due to that the most severe time delay existing in this system is 10 s, the coincidence horizon $N_1=2$ samples is imposed. The control horizon is chosen as $N_u=1$ in this study. The dynamics are different for sub-loops in this system, so different prediction horizon sets are applied; by only changing these, we can then conclude upon its effects on the overall system performance. The analysed cases with different prediction horizon values are described as follows:

Case 1: $N_{21},...,N_{25}=15$ samples;

Case 2 : $N_{21}=N_{24}=N_{25}=20$ samples and $N_{22}=N_{23}=15$ samples ;

Case 3: $N_{21},...,N_{25}=20$ samples.

The performance of NEPSAC on steam/water loop for each of these cases are shown in Fig. 4 and Fig. 5, respectively. Fig. 4 indicates that the system outputs are almost the same with different prediction horizon sets. However, the control efforts are aggressive for the case 1 and case 3 where there are the same prediction horizon for each sub-loop as shown in Fig. 5, while the control efforts change gently for case 2.

In order to test which case provides the best result, performance indexes are compared including Integrated Absolute Relative Error (*IARE*), Integral Secondary control output (*ISU*), Ratio of Integrated Absolute Relative Error (*RIARE*), Ratio of Integral Secondary control output (*RISU*), Number of Iterations (*NOI*) and combined index (*J*). These indexes can be calculated as the following expressions, where the values of w_1 and w_2 in (15) are chosen as $w_1=0.5$, $w_2=0.5$:

$$IARE_i = \sum_{k=0}^{N} \left| r_i(k) - y_i(k) \right| \Big/ r_i(k) \quad (i=1,2,...,5) \qquad (11)$$

Fig. 4. System outputs with NEPSAC controller for the three cases of tuning prediction horizon sets in the five sub-loops.
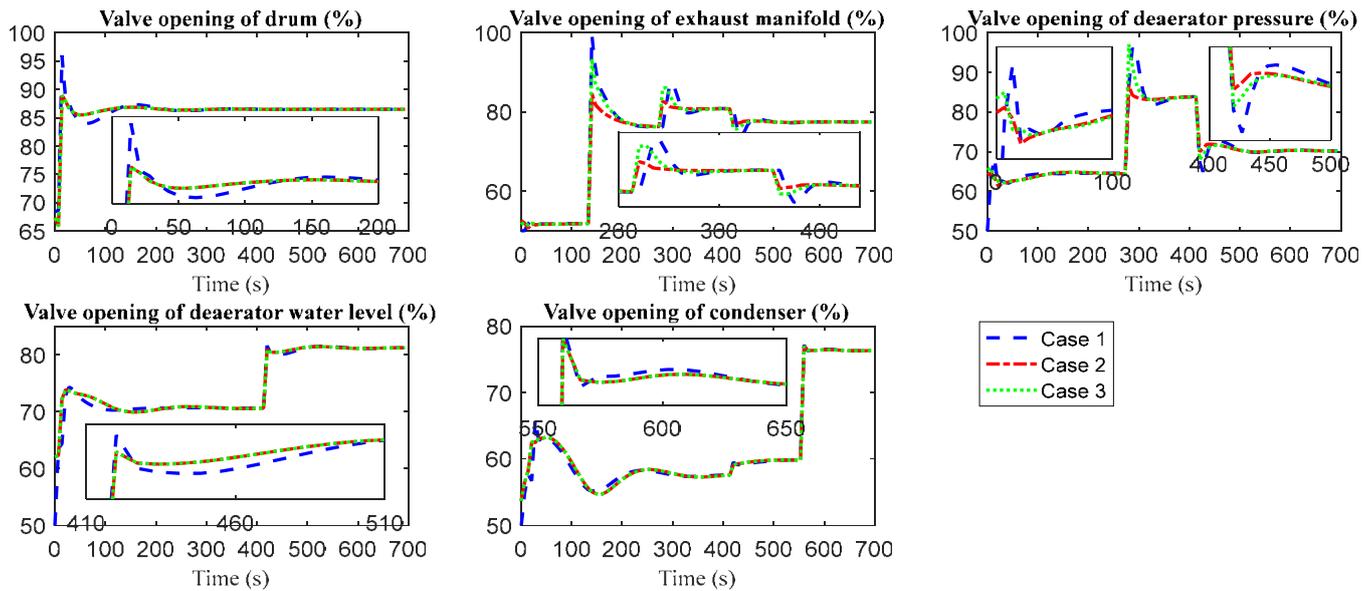
Fig. 5. Control effort corresponding to the three cases with different prediction horizon values

$$ISU_i = \sum_{k=0}^{N} (u_i(k) - u_{ssi}(k))^2 \quad (i=1,2,...,5) \qquad (12)$$

where u_{ssi} is steady state value of ith input;

$$RIARE_i(C_2, C_1) = \frac{IARE_i(C_2)}{IARE_i(C_1)} \quad (i=1,2,...,5) \qquad (13)$$

$$RISU_i(C_2, C_1) = \frac{ISU_i(C_2)}{ISU_i(C_1)} \quad (i=1,2,...,5) \qquad (14)$$

$$J(C_2, C_1) = \frac{1}{5}\sum_{i=1}^{5} \frac{w_1 RIARE_i(C_2,C_1) + w_2 RISU_i(C_2,C_1)}{w_1 + w_2} \qquad (15)$$

According to the numerical values shown in Table 2 and Table 3, the outputs errors are close to each other among the three cases. However, as indicated by *RISU*, the control action changes greater in case 1 and case 3 than that in case 2. It can be observed from index *NOI* that number of iterations is low, their computational time remaining well within the chosen sampling period. As indicated by the performance index *J*, case 2 has the best performance, and case 1 has the worst performance.

Table 2. Performance indexes for IARE, ISU and NOI

Index	Predictive Horizon	Case 1	Case 2	Case 3
IARE	Sub-loop 1	1.0447	1.2162	1.2162
	Sub-loop 2	0.6159	0.7891	0.6436
	Sub-loop 3	0.5481	0.6827	0.5698
	Sub-loop 4	1.5810	2.0864	2.0864
	Sub-loop 5	2.7280	2.9644	2.9644
ISU	Sub-loop 1	0.0137	0.0016	0.0016
	Sub-loop 2	1.1791	0.3274	0.7987
	Sub-loop 3	0.5036	0.3743	0.4607
	Sub-loop 4	0.5125	0.1929	0.1929
	Sub-loop 5	0.5255	0.4551	0.4551
NOI		107	119	120

4.2 Robustness of the NEPSAC Method

In order to test the robustness of the NEPSAC method, step tests over the entire operating range are imposed. Among the five sub-loops in steam/water loop, the drum water level control loop has the most strong interaction with other loops. Hence, robustness test are performed in this sub-loop. Fig. 6 shows the results in robustness test for drum water level control loop. From the results, the NEPSAC method has good performance not only at the operation points, but as expected, it works well within the entire operating range.

Table 3. Performance indexes for RIARE, RISU and J

Index		Case 2 vs Case 1	Case 3 vs Case 2	Case 3 vs Case 1
RIARE	Sub-loop 1	1.1642	1	1.1642
	Sub-loop 2	1.2812	0.8156	1.0450
	Sub-loop 3	1.2456	0.8346	1.0396
	Sub-loop 4	1.3197	1	1.3197
	Sub-loop 5	1.0867	1	1.0867
RISU	Sub-loop 1	0.1168	1	0.1168
	Sub-loop 2	0.2777	2.4395	0.6774
	Sub-loop 3	0.7432	1.2308	0.9148
	Sub-loop 4	0.3764	1	0.3764
	Sub-loop 5	0.8660	1	0.8660
J		0.8477	1.1321	0.8606

5. CONCLUSIONS

In this paper, a nonlinear model predictive control named NEPSAC is applied to the complex steam/water loop. By using iterations, the superposition principle is bypassed in this method, which makes it applicable for nonlinear systems. Due to the different dynamics of the sub-loops of the multivariable system, different prediction horizon sets are applied. The simulation results indicate the trade-off between control effort and performance is better with tailored values than with common value for each sub-loop. A next step is to investigate whether the effect of larger control horizon $N_u > 1$ sample will further improve the performance.
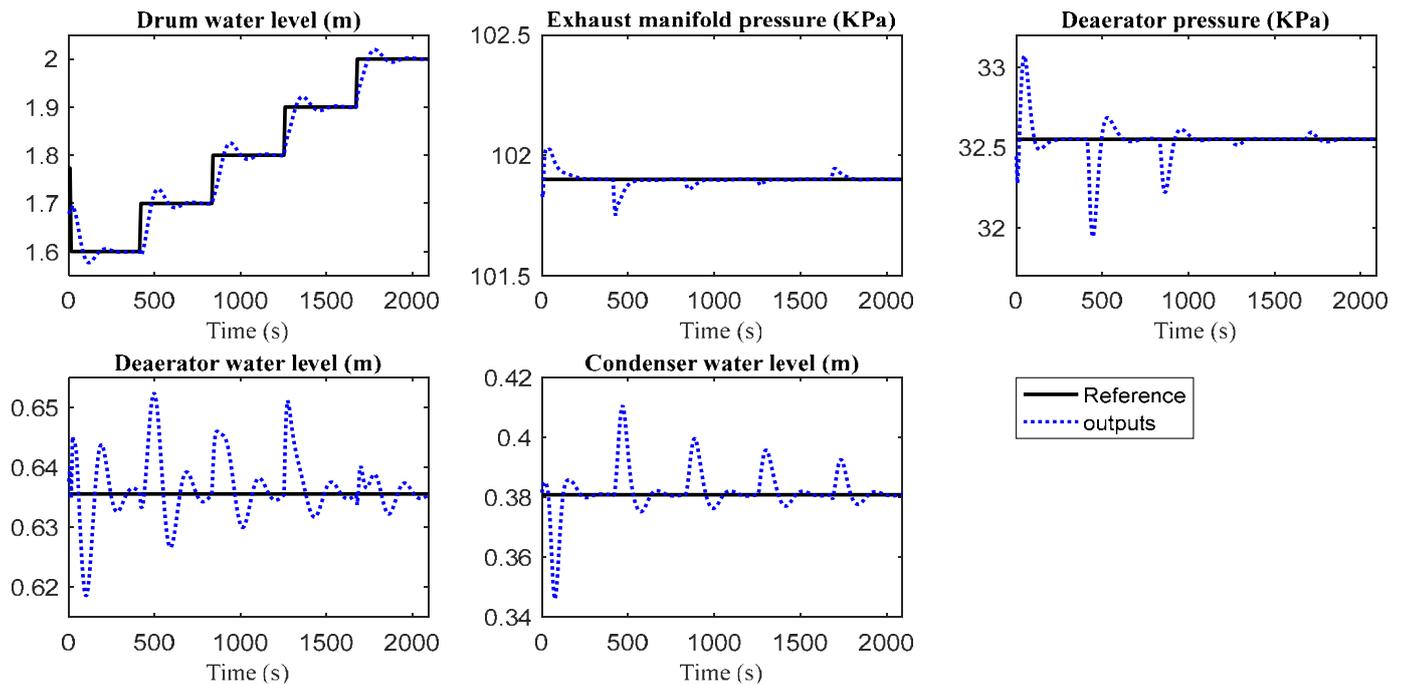
Fig. 6. Robustness test on drum water level control loop

REFERENCES

Åström, K.J. and Bell, R.D. (2000). Drum-boiler dynamics. *Automatica*, 36(3), 363378.

Castano, J. A., Hernandez, A., Li, Z., Tsagarakis, N. G., Caldwell, D. G., and De Keyser, R. (2015). Enhancing the robustness of the EPSAC predictive control using a Singular Value Decomposition approach. *Robotics and Autonomous Systems*, 74, 283-295.

Debert, M., Yhamaillard, G., and Ketfi-herifellicaud, G.A. (2010). Predictive energy management for hybrid electric vehicles-prediction horizon and battery capacity sensitivity. *IFAC Proceedings Volumes*, 43(7), 270-275.

Folea, S. C., Moiş, G., Muresan, C. I., Miclea, L., De Keyser, R., and Cirstea, M. N. (2016). A portable implementation on industrial devices of a predictive controller using graphical programming. *IEEE Transactions on Industrial Informatics*, 12(2), 736-744.

Hernandez, A., Desideri, A., Ionescu, C., De Keyser, R., Lemort, V., and Quoilin, S. (2016). Real-time optimization of organic rankine cycle systems by extremum-seeking control. *Energies*, 9(5), 334.

Kong, X., Liu, X., and Lee, K.Y. (2015). Nonlinear multivariable hierarchical model predictive control for boiler-turbine system. *Energy*, 93, 309-322.

Ławryńczuk, M. (2017). Nonlinear predictive control of a boiler-turbine unit: A state-space approach with successive on-line model linearisation and quadratic optimisation. *ISA transactions*, 67, 476-495.

Liu, X. (2006). *Ship power plant*, China Communications Press, China.

Liu, X. and Cui, J. (2018). Economic model predictive control of boiler-turbine system. *Journal of Process Control*, 66, 59-67.

Morari, M., and Lee, J. H. (1999). Model predictive control: past, present and future. *Computers and Chemical Engineering*, 23(4-5), 667-682.

Sindareh-Esfahani, P., Tabatabaei, S.S., and Pieper, J.K. (2017). Model predictive control of a heat recovery steam generator during cold start-up operation using piecewise linear models. *Applied Thermal Engineering*, 119, 516-529.

Wang, P., Liu, M., and Ge, X. (2014). Study of the improvement of the exhaust steam maniline pressure control system of a steam-driven power plant. *Journal of Engineering for Thermal Energy and Power*, 29(1), 65-70.

Wang, P., Meng, H., Dong, P., and Dai, R. (2015). Decoupling control based on pid neural network for deaerator and condenser water level control system. *In 34th CCC Chinese Control Conference*, 3441-3446. IEEE.

Wu, X., Shen, J., Li, Y., and Lee, K.Y. (2014). Hierarchical optimization of boiler-turbine unit using fuzzy stable model predictive control. *Control Engineering Practice*, 30, 112-123.

Yu, N., Ma, W., and Su, M. (2006). Application of adaptive grey predictor based algorithm to boiler drum level control. *Energy conversion and management*, 47(18-19), 2999-3007.